Chemical Science International Journal

27(4): 1-19, 2019; Article no.CSIJ.50645
ISSN: 2456-706X
(Past name: American Chemical Science Journal, Past ISSN: 2249-0205)

Selective Alteration of the Root Morphology of *Arabidopsis thaliana* by Synthetic Anion Transporters (SATs)

Mohit B. Patel[1,2], Evan C. Garrad[2], Steven Korb[2], Saeedeh Negin[1], Michael R. Gokel[1], Sergey Sedinkin[1], Shanheng Yin[1] and George W. Gokel[1,2*]

[1]Department of Chemistry and Biochemistry, University of Missouri – St. Louis, 1 University Blvd., St. Louis, MO 63121, USA.
[2]Department of Biology, University of Missouri – St. Louis, 1 University Blvd., St. Louis, MO 63121, USA.

Authors' contributions

This work was carried out in collaboration among all authors. Authors MBP and GWG designed the study, performed the statistical analyses, performed the literature searches and wrote the first draft of the manuscript. Syntheses were conducted by authors SS and SY. The plant growth studies were conducted by authors ECG, MRG and SK. Ion release studies were conducted by author SN. All authors read and approved the final manuscript.

Article Information

DOI: 10.9734/CSJI/2019/v27i430119
Editor(s):
(1) Dr. Yunjin Yao, School of Chemical Engineering, Hefei University of Technology, China.
Reviewers:
(1) R. Mahalakshmi, India.
(2) Paul Benyamin Timotiwu, University of Lampung, Indonesia.
Complete Peer review History: http://www.sdiarticle3.com/review-history/50645

Original Research Article

Received 01 June 2019
Accepted 07 August 2019
Published 13 August 2019

ABSTRACT

Aims: The aim of the study was to determine whether and to what extent any of a family of amphiphilic heptapeptide synthetic anion transporters (SATs) affected the growth or root morphology of *Arabidopsis thaliana*.
Study Design: *A. thaliana* plants were grown from seedlings in PNS media in the absence or presence of one of 21 SATs.
Place and Duration of Study: Departments of Chemistry & Biochemistry, University of Missouri – St. Louis, 1 University Blvd., St. Louis, MO 63121 U. S. A. The study was conducted 2017-2018.

**Corresponding author: E-mail: gokelg@umsl.edu, ggokel@fastmail.fm;*

Methodology: Twenty one compounds of the form R_2N-$COCH_2YCH_2CO$-$(Aaa)_3Pro(Aaa)_3$-$O(CH_2)_6CH_3$ were prepared and studied. The amino acids included Ala, Gly, and Ser. R was normal alkyl having 6, 10, 12, or 18 carbons. Y was methylene, oxygen, sulfur, or absent. The PNS media was infused with various concentrations of the SAT and 21 plants in each group were allowed to grow for 11 days. Overall plant growth and root morphology were visualized and/or measured and the results recorded.
Results: A comparison of primary root length and lateral root number revealed that the greatest alterations in lateral root densities were observed for peptide sequences of the type GGGPSGS, whether or not serine was protected by *t*-butyl. Differences were also observed for these peptide sequences according to the identity of Y in the ~$COCH_2YCH_2CO$~ chain.
Conclusion: The presence of serine's oxygen atoms on the C-terminal side of the heptapeptide interact with Cl^- leading to a change in ion concentrations and alterations in primary root lengths and lateral root densities.

Keywords: Amphiphile; Arabidopsis thaliana; heptapeptide; lateral root density; synthetic anion transporter; synthetic ion channel.

1. INTRODUCTION

During recent decades, extensive study has been reported of biological effects of ion binders and transporters, particularly of cation complexers on bacteria and fungi. [1-2] Within the crown ether class of ion binders and transporters, biological effects have been reported involving microbes, [3-15] tissues, [16-22] plants, [23-27] and animals. [16-22] Although several reports relate to studies of whole plants, this remains a poorly explored area.

We recently reported the effect of hydraphile and lariat ether synthetic cation transporters on the growth of *Arabidopsis thaliana*. [28-30] These cation binders and transporters showed significant effects on *A. thaliana* root morphology. The effect mimicked the action of the growth hormone indoleacetic acid, albeit at a much higher concentration than observed with the natural hormone. More detailed study revealed that the transporters were not true growth hormone mimics. Our surmise was that the observed behavior related to changes in ion balance mediated to greater or lesser extents by the efficacy of the transporter.

Although only limited studies have been reported of interactions between alkali metal ion carriers and/or transporters, factors affecting root morphology has been an area of interest for some time. This includes studies of root alterations caused by chemical excesses or deficiencies in maize, [31] in *Medicago sativa L.*, [32] and the Brazilian medicinal plant *Pfaffia glomerata*. [33] In the latter case, the presence of zinc metal was the focus of study. Notwithstanding, research on the interactions of alkali metal ion binders such as cryptands and crown ethers with vital plants are almost unknown. Other recent studies include examinations of copper toxicity to grapevine [34] and cation effects on banana root segments. [35] The effect of the polyamine cadaverine on *A. thaliana* has recently been reported [36].

The class of compounds we have called synthetic anion transporters (SATs) [37] were designed and confirmed to transport Cl^- through phospholipid bilayer membranes. [38] The SATs were designed based on the putative chloride selectivity sequence of the ClC family of proteins. This led to the selection of G_3PG_3 peptide sequence. [39] Since the peptide must insert in membranes, an anchoring module was added to the N-terminal end of the peptide. The initial module was $[CH_3(CH_2)_{17}]_2N$. Reaction of the secondary amine with diglycolic anhydride produced the entire anchor module, $(C_{18}H_{37})_2NCOCH_2OCH_2COOH$ in a single step. This module corresponds in dimension and polarity to the corresponding segment of distearoylphosphatidylcholine. Heptanol was determined by experiment to be the most effective C-terminal secondary anchor that would also block the unlinked glycine carboxyl [40].

The SATs show Cl^--selective release from liposomes and open-close behavior characteristic of protein chloride channels. [41] When the anchor chains were C_{18}, Cl^- ion selectivity was high, but it diminished as the primary anchor chains were shortened. [42] The original diglycolic acid module was replaced by glutaric acid, succinic acid, and thiodiglycolic acid.

[43] Surprisingly, SATs containing succinic acid proved to be the most active ion transporters. Biophysical studies confirmed membrane insertion and the formation of a dimeric pore [44].

To our knowledge, previous studies of effects on plants by ion binding agents [4,25] focused on the complexation and/or transport of cations, specifically sodium and potassium, that could affect plant growth dynamics. The investigation reported here was initiated to discover if and to what extent altering anion balance, in particular Cl^-, would affect root morphology or any other plant phenotype. The results of those studies follow.

2. MATERIALS AND METHODS

2.1 General

^{1}H-NMR were recorded at 300 MHz in $CDCl_3$ solvents and are reported in ppm (*delta*) downfield from internal $(CH_3)_3Si$. ^{13}C-NMR were recorded at corresponding frequencies in $CDCl_3$ unless otherwise stated. Melting points were determined on a Thomas Hoover apparatus in open capillaries and are uncorrected. Thin layer chromatographic (TLC) analyses were performed on aluminum oxide 60 F-254 neutral (Type E) with a 0.2 mm layer thickness or on silica gel 60 F-254 with a 0.2 mm layer thickness. Preparative chromatography columns were packed with activated aluminum oxide (MCB 80-325 mesh, chromatographic grade, AX 611) or with Kieselgel 60 (70-230 mesh). All reactions were conducted under dry N_2 unless otherwise stated. All reagents were the best (non-LC) grade commercially available and were distilled, recrystallized, or used without further purification, as appropriate.

2.2 Preparation of $(C_6H_{13})_2NCOCH_2CH_2CO(Gly)_3Pro(Gly)_3$-$OC_7H_{15}$, 1

$(C_6H_{13})_2NCOCH_2CH_2CO(Gly)_3OH$ (160 mg, 0.350 mmol) was dissolved in DMF (5 mL) in a 25 mL rb flask. The mixture was cooled to 0 °C and 2,4,6-trimethylpyridine (140 µL) and HBTU (140 mg) were added. The mixture was stirred for 30 min and H-Pro(Gly)$_3$-OC_7H_{15} (150 mg) was added. The mixture was stirred at rt for 16 h. The mixture was diluted with CH_2Cl_2 (250 mL) and washed with 250 mL each of the following: H_2O, 1*M* $NaHSO_4$, H_2O × 3, 5% $NaHCO_3$, and H_2O. The CH_2Cl_2 solution was filtered through a 1:1 celite/$MgSO_4$ mixture. The solution was evaporated and chromatographed over a column of SiO_2 (eluent: 0%-20% MeOH in $CHCl_3$). Evaporation of the solvent followed by high vacuum for 16 h afforded **1** as a white solid (243 mg, 84% yield). MP: 85-90ºC. ^{1}H NMR: 0.8 (t, 9H); 1.19 (m, 20H); 1.37 (bs, 3H); 1.61 (bs, 3H); 2.37 (t, 2H); 2.74 (t, 2H); 3.14 (t, 4H); 3.89 (m, 8H); 4.08 (m, 2H); 6.48 (s, 1H); 7.02 (s, 1H); 8.12 (s, 1H) ppm.

2.3 Preparation of $(C_{10}H_{21})_2NCOCH_2CH_2CO(Gly)_3Pro(Gly)_3$-$OC_7H_{15}$, 2

$(C_{10}H_{21})_2NCOCH_2CH_2CO(Gly)_3OH$ (300 mg, 0.527 mmol) was dissolved in DMF (5 mL) in a 25 mL rb flask. The mixture was cooled to 0 °C and 2,4,6-trimethylpyridine (210 µL) and HBTU (210 mg) were added. The mixture was stirred for 30 min and H-Pro(Gly)$_3$-OC_7H_{15} (222 mg) was added. The mixture was stirred at rt for 16 h. The mixture was diluted with CH_2Cl_2 (250 mL) and washed with 250 mL each of the following: H_2O, 1M $NaHSO_4$, H_2O × 3, 5% $NaHCO_3$, and H_2O. The CH_2Cl_2 solution was filtered through a 1:1 celite/$MgSO_4$ mixture. The solution was evaporated and chromatographed over a column of SiO_2 (eluent: 0%-20% MeOH in $CHCl_3$). Evaporation of the solvent followed by high vacuum for 16 h afforded **2** as a white solid (433 mg, 88% yield). MP: 147-152ºC. ^{1}H NMR: 0.81 (t, 9H); 1.17 (bs, 36H); 1.36 (bs, 2H); 1.55 (bs, 4H); 1.93-2.14 (m, 4H); 2.33 (m, 1H); 2.57 (m, 2H); 2.75 (m, 1H); 3.13 (bs, 4H); 3.62 (m, 6H); 3.85 (d, 1H); 4.16 (m, 8H); 7.35 (bs, 2H); 7.46 (bs, 1H); 7.89 (bs, 1H); 8.17 (bs, 1H) ppm.

2.4 Preparation of $(C_{12}H_{23})_2NCOCH_2CH_2CO(Gly)_3Pro(Gly)_3$-$OC_7H_{15}$, 3

$(C_{12}H_{23})_2NCOCH_2CH_2CO(Gly)_3OH$ (300 mg, 0.480 mmol) was dissolved in DMF (5 mL) in a 25 mL rb flask. The mixture was cooled to 0ºC and 2,4,6-trimethylpyridine (190 µL) and HBTU (191 mg) were added. The mixture was stirred for 30 min and H-Pro(Gly)$_3$-OC_7H_{15} (202 mg) was added. The mixture was stirred at rt for 16 h. The mixture was diluted with CH_2Cl_2 (250 mL) and washed with 250 mL each of the following: H_2O, 1M $NaHSO_4$, H_2O × 3, 5% $NaHCO_3$, and H_2O. The CH_2Cl_2 solution was filtered through a 1:1 celite/$MgSO_4$ mixture. The solution was evaporated and chromatographed over a column of SiO_2 (eluent: 0%-20% MeOH in $CHCl_3$).

Evaporation of the solvent followed by high vacuum for 16 h afforded **3** as a white solid (412 mg, 86% yield). MP: 147-151ºC. ^{1}H NMR: 0.92 (t, 9H); 1.29 (bs, 44H); 1.47 (bs, 2H); 1.65 (bs, 4H); 2.04 (s, 2H); 2.25 (m, 2H); 2.39 (m, 2H); 2.44 (m, 1H); 2.60-2.80 (m, 2H); 2.90 (m, 1H); 3.24 (bs, 4H); 3.62 (m, 6H); 3.97 (d, 1H); 4.14 (m, 8H); 7.44 (bs, 3H); 8.03 (bs, 1H); 8.29 (bs, 1H) ppm.

2.5 Preparation of $(C_{18}H_{37})_2NCOCH_2CH_2CO(Gly)_3Pro(Gly)_3$-$OC_7H_{15}$, 4

$(C_{18}H_{37})_2NCOCH_2CH_2CO(Gly)_3OH$ (309 mg, 0.390 mmol) and 184 mg H-Pro$(Gly)_3$-OC_7H_{15} were dissolved in CH_2Cl_2 (5 mL containing 64 mg *n*-butanol) in a 25 mL rb flask. The mixture was cooled to 0ºC and EDCI (81 mg) and triethylamine (0.21 mL) were added. The mixture was stirred at rt under argon for 16 h. The mixture was diluted with CH_2Cl_2 (100 mL) and washed with 100 mL each of the following: H_2O, 1M $NaHSO_4$, H_2O, 5% $NaHCO_3$, and H_2O. The CH_2Cl_2 solution was filtered through a 1:1 celite/$MgSO_4$ mixture. The solution was evaporated and chromatographed over a column of SiO_2 (eluent: 5%-15% MeOH in $CHCl_3$. Evaporation followed by high vacuum for 16 h afforded **4** as a white solid (356 mg, 79% yield). MP: 148-152ºC. ^{1}H NMR: 0.87 (m, 12H), 1.25 (m, 72H), 1.42 (br s, 2H), 1.55 (br s, 2H), 1.80–2.40 (m, 4H), 2.40–2.80 (m, 4H), 3.22 (br s, 4H), 3.25–4.40 (m, 15H), 7.45 (br s, 2H), 7.73 (br s, 1H), 8.14 (s, 2H).

2.6 Preparation of $(C_6H_{13})_2NCOCH_2OCH_2CO(Gly)_3Pro(Gly)_3$-$OC_7H_{15}$, 5

Preparation of $(C_6H_{13})_2NCOCH_2OCH_2CO(Gly)_3Pro(Gly)_3$-$OC_7H_{15}$, **5** was prepared as previously reported [38].

2.7 Preparation of $(C_{18}H_{37})_2NCOCH_2OCH_2CO(Gly)_3Pro(Gly)_3$-$OC_7H_{15}$, 6

Preparation of $(C_{18}H_{37})_2NCOCH_2OCH_2CO(Gly)_3Pro(Gly)_3$-$OC_7H_{15}$, **6** was prepared as previously reported [40].

2.8 Preparation of $(C_{12}H_{23})_2NCOCH_2CH_2CO(Ala)_3Pro(Gly)_3$-$OC_7H_{15}$, 7

$(C_{12}H_{23})_2NCOCH_2CH_2CO(Ala)_3OH$ (62 mg, 0.093 mmol) and 82 mg H-Pro$(Gly)_3$-OC_7H_{15} were dissolved in DMF (5 mL) in a 25 mL rb flask. The mixture was cooled to 0ºC and 2,4,6-trimethylpyridine (55 µL) and HBTU (55 mg) were added. The mixture was stirred at rt for 16 h. The mixture was diluted with CH_2Cl_2 (150 mL) and washed with 150 mL each of the following: H_2O, 1M $NaHSO_4$, H_2O × 3, 5% $NaHCO_3$, and H_2O. The CH_2Cl_2 solution was filtered through a 1:1 celite/$MgSO_4$ mixture. The solution was evaporated and chromatographed over a column of SiO_2 (eluent: 0%-10% MeOH in $CHCl_3$. Evaporation of the solvent followed by high vacuum for 16 h afforded **7** as a white solid (101 mg, 71% yield). MP: 130-135ºC. ^{1}H NMR: 0.81 (t, 13H); 1.19 (bs, 73H); 1.40 (bs, 15H); 1.84-2.16 (m, 6H); 2.34 (s, 2H); 2.61 (m, 3H); 2.80-3.16 (m, 7H); 3.57 (m, 3H); 3.90 (m, 9H); 4.28 (m, 5H); 6.15 (d, 1H); 7.50 (t, 1H); 7.68 (d, 1H); 7.86 (t, 1H) ppm.

2.9 Preparation of $(C_{18}H_{37})_2NCOCH_2CH_2CO(Ala)_3Pro(Gly)_3$-$OC_7H_{15}$, 8

$(C_{18}H_{37})_2NCOCH_2CH_2CO(Ala)_3OH$ (62 mg, 0.102 mmol) and 82 mg H-Pro$(Gly)_3$-OC_7H_{15} were dissolved in DMF (5 mL) in a 25 mL rb flask. The mixture was cooled to 0ºC and 2,4,6-trimethylpyridine (55 µL) and HBTU (55 mg) were added. The mixture was stirred at rt for 16 h. The mixture was diluted with CH_2Cl_2 (150 mL) and washed with 150 mL each of the following: H_2O, 1M $NaHSO_4$, H_2O × 3, 5% $NaHCO_3$, and H_2O. The CH_2Cl_2 solution was filtered through a 1:1 celite/$MgSO_4$ mixture. The solution was evaporated and chromatographed over a column of SiO_2 (eluent: 0%-10% MeOH in $CHCl_3$. Evaporation of the solvent followed by high vacuum for 16 h afforded 8 as a white solid (120 mg, 73% yield). MP: 153-157ºC. ^{1}H NMR: 0.92 (t, 12H); 1.31 (bs, 96H); 1.49 (bs, 14H); 1.94-2.26 (m, 7H); 2.45 (s, 2H); 2.71 (m, 2H); 3.25-3.33 (m, 7H); 3.71 (m, 3H); 4.39-4.54 (m, 14H); 6.37 (d, 1H); 7.31 (t, 2H); 7.75 (d, 2H); 8.00 (t, 1H) ppm.

2.10 Preparation of $(C_{12}H_{23})_2NCOCH_2OCH_2CO(Ala)_3Pro(Gly)_3$-$OC_7H_{15}$, 9

$(C_{12}H_{23})_2NCOCH_2OCH_2CO(Ala)_3OH$ (186 mg, 0.272 mmol) and 237 mg H-Pro$(Gly)_3$-OC_7H_{15} were dissolved in DMF (5 mL) in a 25 mL rb flask. The mixture was cooled to 0ºC and 2,4,6-trimethylpyridine (160 µL) and HBTU (160 mg) were added. The mixture was stirred at rt for 16 h. The mixture was diluted with CH_2Cl_2 (150 mL) and washed with 150 mL each of the following:

H_2O, 1M $NaHSO_4$, H_2O × 3, 5% $NaHCO_3$, and H_2O. The CH_2Cl_2 solution was filtered through a 1:1 celite/$MgSO_4$ mixture. The solution was evaporated and chromatographed over a column of SiO_2 (eluent: 0%-10% MeOH in $CHCl_3$. Evaporation of the solvent followed by high vacuum for 16 h afforded **9** as a white solid (101 mg, 71% yield). MP: 128-134ºC. ^{1}H NMR: 0.92 (t, 9H); 1.29 (bs, 54H); 1.50 (m, 10H); 2.16 (m, 6H); 3.11-3.82 (m, 6H); 4.11 (m, 8H); 4.51 (m, 7H); 7.31 (m, 2H); 7.66 (d, 2H); 7.85 (d, 1H); 7.99 (t, 1H) ppm.

2.11 Preparation of $(C_{18}H_{37})_2NCOCH_2OCH_2CO(Ala)_3Pro(Gly)_3$-$OC_7H_{15}$, 10

$(C_{18}H_{37})_2NCOCH_2OCH_2CO(Ala)_3OH$ (253 mg, 0.297 mmol) and 237 mg H-$Pro(Gly)_3$-OC_7H_{15} were dissolved in DMF (5 mL) in a 25 mL rb flask. The mixture was cooled to 0 °C and 2,4,6-trimethylpyridine (160 µL) and HBTU (160 mg) were added. The mixture was stirred at rt for 16 h. The mixture was diluted with CH_2Cl_2 (150 mL) and washed with 150 mL each of the following: H_2O, 1*M* $NaHSO_4$, H_2O × 3, 5% $NaHCO_3$, and H_2O. The CH_2Cl_2 solution was filtered through a 1:1 celite/$MgSO_4$ mixture. The solution was evaporated and chromatographed over a column of SiO_2 (eluent: 0%-10% MeOH in $CHCl_3$. Evaporation of the solvent followed by high vacuum for 16 h afforded **10** as a white solid (409 mg, 85% yield). MP: 126-130ºC. ^{1}H NMR: 0.80 (t, 10H); 1.18 (bs, 85H); 1.38 (bs, 10H); 1.87 (m, 2H); 2.06 (bs, 7H); 2.99 (m, 4H); 3.53 (m, 2H); 3.81 (m, 10H); 4.23 (m, 8H); 7.20 (m, 2H); 7.57 (d, 1H); 7.67 (t, 1H); 7.75 (d,1H); 7.90 (t, 1H) ppm.

2.12 Preparation of $(C_{18}H_{37})_2NCOCH_2SCH_2CO(Ala)_3Pro(Gly)_3$-$OC_7H_{15}$, 11

$(C_{18}H_{37})_2NCOCH_2SCH_2CO(Ala)_3OH$ (127 mg, 0.297 mmol) and 116 mg H-$Pro(Gly)_3$-OC_7H_{15} were dissolved in DMF (5 mL) in a 25 mL rb flask. The mixture was cooled to 0ºC and 2,4,6-trimethylpyridine (50 µL) and HBTU (77 mg) were added. The mixture was stirred at rt for 16 h. The mixture was diluted with CH_2Cl_2 (150 mL) and washed with 150 mL each of the following: H_2O, 1M $NaHSO_4$, H_2O × 3, 5% $NaHCO_3$, and H_2O. The CH_2Cl_2 solution was filtered through a 1:1 celite/$MgSO_4$ mixture. The solution was evaporated and chromatographed over a column of SiO_2 (eluent: 0%-10% MeOH in $CHCl_3$. Evaporation of the solvent followed by high vacuum for 16 h afforded **11** as a white solid (183 mg, 76% yield). MP: 154-158ºC. ^{1}HNMR: 0.88 (t, 9H); 1.28 (bs, 68H); 1.39 (bs, 2H); 1.65 (bs, 4H); 1.97-2.17 (s, 4H); 2.95-4.10 (m, 18H); 4.38 (m, 3H); 4.66 (m, 1H); 7.48 (bs, 2H); 7.65 (bs, 1H); 8.01 (bs, 1H); 8.14 (bs, 2H) ppm.

2.13 Preparation of $(C_{12}H_{23})_2NCOCH_2CH_2CO(Gly)_3ProSerGlySer$-$OC_7H_{15}$, 12

$(C_{12}H_{23})_2NCOCH_2CH_2CO(Gly)_3ProGlySer(t$-Bu)Gly-$OC_7H_{15}$ (205 mg, 0.195 mmol) was dissolved in dioxane (2 mL). The mixture was cooled and stirred to 0ºC and 4M HCl in dioxane (1 mL) was added. The mixture was stirred at 0 °C for 2 h. The solvent was evaporated followed by high vacuum for 16 h afforded **12** as a white solid (160 mg, 80% yield). MP: 129-134 °C. ^{1}H NMR: 0.80 (t, 10H); 1.07 (s, 4H); 1.21 (bs, 68H); 1.36 (bs, 6H); 1.91-2.43 (m, 10H); 3.13 (bs, 4H); 3.48-4.10 (m, 17H); 4.53 (m, 1H); 7.40-8.40 (m, 6H) ppm.

2.14 Preparation of $(C_{18}H_{37})_2NCOCH_2CH_2CO(Gly)_3ProSerGlySer$-$OC_7H_{15}$, 13

$(C_{18}H_{37})_2NCOCH_2CH_2CO(Gly)_3ProSer(t$-Bu)GlySer(*t*-Bu)-$OC_7H_{15}$ (200 mg, 0.164 mmol) was dissolved in Dioxane (2 mL). The mixture was cooled and stirred to 0ºC and 4M HCl in dioxane (1 mL) was added. The mixture was stirred at 0ºC for 2 h. The solvent was evaporated followed by high vacuum for 16 h afforded **13** as a white solid (146 mg, 75%). MP: 145-150ºC. ^{1}H NMR: 0.80 (t, 10H); 1.07 (s, 4H); 1.21 (bs, 68H); 1.36 (bs, 6H); 1.91-2.43 (m, 10H); 3.13 (bs, 4H); 3.48-4.10 (m, 17H); 4.53 (m, 1H); 7.40-8.40 (m, 6H) ppm.

2.15 Preparation of $(C_{18}H_{37})_2NCOCH_2OCH_2CO(Gly)_3ProSerGlySer$-$OC_7H_{15}$, 14

$(C_{18}H_{37})_2NCOCH_2OCH_2CO(Gly)_3ProSer(t$-Bu)GlySer(*t*-Bu)-$OC_7H_{15}$ (200 mg, 0.162 mmol) was dissolved in dioxane (2 mL). The mixture was cooled and stirred to 0ºC and 4M HCl in dioxane (1 mL) was added. The mixture was stirred at 0ºC for 2 h. The solvent was evaporated, followed by high vacuum for 16 h afforded **14** as a white solid (165 mg, 85%). MP: 74-78ºC. ^{1}H NMR: 0.80 (t, 10H); 1.08 (s, 4H); 1.18 (bs, 68H); 1.44 (d, 6H); 1.96 (bs, 10H); 3.00 (m, 2H); 3.20 (bs, 2H); 3.46 (bs, 1H); 3.91 (m, 10H); 4.22 (m, 4H); 7.40-8.49 (m, 6H) ppm.

2.16 Preparation of $(C_{12}H_{23})_2NCOCH_2CH_2CO(Gly)_3ProSer(t\text{-}Bu)GlySer(t\text{-}Bu)\text{-}OC_7H_{15}$, 15

$(C_{12}H_{23})_2NCOCH_2CH_2CO(Gly)_3OH$ (224 mg, 0.358 mmol) and 200 mg H-ProSer(t-Bu)GlySer(t-Bu)-OC_7H_{15} were dissolved in DMF (10 mL) in a 25 mL rb flask. The mixture was cooled to 0ºC and 2,4,6-trimethylpyridine (140 µL) and HBTU (143 mg) were added. The mixture was stirred at rt for 16 h. The mixture was diluted with CH_2Cl_2 (150 mL) and washed with 150 mL each of the following: H_2O, 1M $NaHSO_4$, H_2O × 3, 5% $NaHCO_3$, and H_2O. The CH_2Cl_2 solution was filtered through a 1:1 celite/$MgSO_4$ mixture. The solution was evaporated and chromatographed over a column of SiO_2 (eluent: 0%-10% MeOH in $CHCl_3$). Evaporation of the solvent followed by high vacuum for 16 h afforded **15** as a white solid (375 mg, 90% yield). MP: 109-111ºC. ^{1}H NMR: 0.88 (t, 9H); 1.16 (d, 24H); 1.26 (bs, 44H); 1.45 (bs, 2H); 1.60 (bs, 4H); 2.08 (s, 4H); 2.57 (m, 4H); 3.23 (bs, 4H); 3.57-4.19 (m, 17H); 7.49 (bs, 1H); 7.61 (bs, 1H); 7.75 (bs, 1H); 7.87 (bs, 2H); 8.17 (bs, 1H) ppm.

2.17 Preparation of $(C_{18}H_{37})_2NCOCH_2CH_2CO(Gly)_3ProSer(t\text{-}Bu)GlySer(t\text{-}Bu)\text{-}OC_7H_{15}$, 16

$(C_{18}H_{37})_2NCOCH_2CH_2CO(Gly)_3OH$ (278 mg, 0.350 mmol) and 193 mg H-ProSer(t-Bu)GlySer(t-Bu)-OC_7H_{15} were dissolved in DMF (10 mL) in a 25 mL rb flask. The mixture was cooled to 0 °C and 2,4,6-trimethylpyridine (140 µL) and HBTU (138 mg) were added. The mixture was stirred at rt for 16 h. The mixture was diluted with CH_2Cl_2 (150 mL) and washed with 150 mL each of the following: H_2O, 1M $NaHSO_4$, H_2O × 3, 5% $NaHCO_3$, and H_2O. The dichloromethane solution was filtered through a 1:1 celite/$MgSO_4$ mixture. The solution was evaporated and chromatographed over a column of SiO_2 (eluent: 0%-10% MeOH in $CHCl_3$). Evaporation of the solvent followed by high vacuum for 16 h afforded **16** as a white solid (406 mg, 88% yield). MP: 108-110ºC. ^{1}H NMR: 0.80 (t, 11H); 1.07 (d, 20H); 1.18 (bs, 82H); 1.35 (bs, 3H); 1.50 (m, 5H); 1.94 (m, 7H); 2.37-2.80 (m, 4H); 3.12 (m, 5H); 3.44-4.26 (m, 20H); 4.49 (m, 1H); 6.92 (d, 1H); 7.12 (d, 1H); 7.25 (t, 1H); 7.72 (t, 1H); 7.78 (t, 1H); 8.14 (t, 1H) ppm.

2.18 Preparation of $(C_{12}H_{23})_2NCOCH_2OCH_2CO(Gly)_3ProSer(t\text{-}Bu)GlySer(t\text{-}Bu)\text{-}OC_7H_{15}$, 17

$(C_{12}H_{23})_2NCOCH_2OCH_2CO(Gly)_3OH$ (230 mg, 0.359 mmol) and 200 mg H-ProSer(t-Bu)GlySer(t-Bu)-OC_7H_{15} were dissolved in DMF (10 mL) in a 25 mL rb flask. The mixture was cooled to 0 °C and 2,4,6-trimethylpyridine (140 µL) and HBTU (143 mg) were added. The mixture was stirred at rt for 16 h. The mixture was diluted with CH_2Cl_2 (150 mL) and washed with 150 mL each of the following: H_2O, 1M $NaHSO_4$, H_2O × 3, 5% $NaHCO_3$, and H_2O. The CH_2Cl_2 solution was filtered through a 1:1 celite/$MgSO_4$ mixture. The solution was evaporated and chromatographed over a column of SiO_2 (eluent: 0%-10% MeOH in $CHCl_3$). Evaporation of the solvent followed by high vacuum for 16 h afforded **17** as a white solid (333 mg, 79% yield). MP: 125-128ºC. ^{1}H NMR: 0.88 (t, 9H); 1.16 (d, 18H); 1.26 (bs, 44H); 1.60 (bs, 6H); 2.11 (s, 4H); 3.11 (bs, 2H); 3.28 (bs, 2H); 3.57 (bs, 4H); 3.69 (m, 3H); 4.07 (m, 11H); 4.30 (s, 2H); 4.44 (m, 2H); 4.63 (m, 1H); 7.42 (bs, 2H); 7.71 (bs, 2H); 7.98 (bs, 1H); 8.26 (bs, 1H) ppm.

2.19 Preparation of $(C_{18}H_{37})_2NCOCH_2OCH_2CO(Gly)_3ProSer(t\text{-}Bu)GlySer(t\text{-}Bu)\text{-}OC_7H_{15}$, 18

$(C_{18}H_{37})_2NCOCH_2OCH_2CO(Gly)_3OH$ (281 mg, 0.347 mmol) and 193 mg H-ProSer(t-Bu)GlySer(t-Bu)-OC_7H_{15} were dissolved in DMF (10 mL) in a 25 mL rb flask. The mixture was cooled to 0 °C and 2,4,6-trimethylpyridine (140 µL) and HBTU (138 mg) were added. The mixture was stirred at rt for 16 h. The mixture was diluted with CH_2Cl_2 (150 mL) and washed with 150 mL each of the following: H_2O, 1M $NaHSO_4$, H_2O × 3, 5% $NaHCO_3$, and H_2O. The CH_2Cl_2 solution was filtered through a 1:1 celite/$MgSO_4$ mixture. The solution was evaporated and chromatographed over a column of SiO_2 (eluent: 0%-10% MeOH in $CHCl_3$). Evaporation of the solvent followed by high vacuum for 16 h afforded **18** as a white solid (399 mg, 85% yield). MP: 127-129ºC. ^{1}H NMR: 0.88 (t, 9H); 1.17 (d, 18H); 1.26 (bs, 65H); 1.60 (bs, 6H); 2.08 (bs, 4H); 3.09 (m, 2H); 3.27 (bs, 2H); 3.56-4.62 (m, 25H); 7.41 (m, 1H); 7.63 (bs, 1H); 7.74 (bs, 1H); 7.84 (bs, 1H); 8.09 (bs, 1H); 8.47 (bs, 1H) ppm.

2.20 Preparation of $(C_{12}H_{23})_2NCOCH_2CH_2CO(Gly)_3ProGlySer(t\text{-}Bu)Gly\text{-}OC_7H_{15}$, 19

$(C_{12}H_{23})_2NCOCH_2CH_2CO(Gly)_3OH$ (531 mg, 0.850 mmol) was dissolved in DMF (10 mL) in a 25 mL rb flask. The mixture was cooled to 0 °C and 2,4,6-trimethylpyridine (337 µL) and HBTU (338 mg) were added. The mixture was stirred for 30 min and H-ProGlySer(*t*-Bu)Gly-OC_7H_{15} (400 mg) was added. The mixture was stirred at rt for 16 h. The mixture was diluted with CH_2Cl_2 (250 mL) and washed with 250 mL each of the following: H_2O, 1M $NaHSO_4$, H_2O × 3, 5% $NaHCO_3$, and H_2O. The CH_2Cl_2 solution was filtered through a 1:1 celite/$MgSO_4$ mixture. The solution was evaporated and chromatographed over a column of SiO_2 (eluent: 5%-30% MeOH in $CHCl_3$). Evaporation of the solvent followed by high vacuum for 16 h afforded **19** as a white solid (811 mg, 88% yield). MP: 158-160ºC. ^{1}H NMR: 0.81 (t, 9H); 1.17 (bs, 54H); 1.53 (m, 8H); 1.85 (m, 8H);2.10 (m, 7H); 2.45 (m, 4H); 3.13 (bs, 4H); 3.38-4.05 (m, 17H); 4.39 (m, 2H); 7.07 (d, 1H); 7.31 (bs, 2H); 7.44 (m, 2H); 7.88 (m, 2H) ppm.

2.21 Preparation of $(C_{18}H_{37})_2NCOCH_2CH_2CO(Gly)_3ProGlySer(t\text{-}Bu)Gly\text{-}OC_7H_{15}$, 20

$(C_{18}H_{37})_2NCOCH_2CH_2CO(Gly)_3OH$ (674 mg, 0.850 mmol) was dissolved in DMF (10 mL) in a 25 mL rb flask. The mixture was cooled to 0 °C and 2,4,6-trimethylpyridine (337 µL) and HBTU (338 mg) were added. The mixture was stirred for 30 min and H-ProGlySer(*t*-Bu)Gly-OC_7H_{15} (400 mg) was added. The mixture was stirred at rt for 16 h. The mixture was diluted with CH_2Cl_2 (250 mL) and washed with 250 mL each of the following: H_2O, 1M $NaHSO_4$, H_2O × 3, 5% $NaHCO_3$, and H_2O. The CH_2Cl_2 solution was filtered through a 1:1 celite/$MgSO_4$ mixture. The solution was evaporated and chromatographed over a column of SiO_2 (eluent: 5%-30% MeOH in $CHCl_3$). Evaporation of the solvent followed by high vacuum for 16 h afforded **20** as a white solid (892 mg, 84% yield). MP: 155-158ºC. ^{1}H NMR: 0.88 (t, 11H); 1.16 (s, 13H); 1.26 (bs, 74H); 1.60 (d, 6H); 2.12 (s, 4H); 2.63 (d, 4H); 3.22 (bs, 4H); 3.49-4.15 (m, 18H); 4.50 (bs, 2H); 7.33 (bs, 1H); 7.70 (bs, 3H); 8.12 (bs, 2H) ppm.

2.22 Preparation of $(C_{18}H_{37})_2NCOCH_2OCH_2CO(Gly)_3ProGlySer(t\text{-}Bu)Gly\text{-}OC_7H_{15}$, 21

$(C_{18}H_{37})_2NCOCH_2OCH_2CO(Gly)_3OH$ (515 mg, 0.636 mmol) was dissolved in DMF (10 mL) in a 25 mL rb flask. The mixture was cooled to 0ºC and 2,4,6-trimethylpyridine (337 µL) and HBTU (338 mg) were added. The mixture was stirred for 30 min and H-ProGlySer(t-Bu)Gly-OC_7H_{15} (400 mg) was added. The mixture was stirred at rt for 16 h. The mixture was diluted with CH_2Cl_2 (250 mL) and washed with 250 mL each of the following: H_2O, 1M $NaHSO_4$, H_2O × 3, 5% $NaHCO_3$, and H_2O. The CH_2Cl_2 solution was filtered through a 1:1 celite/$MgSO_4$ mixture. The solution was evaporated and chromatographed over a column of SiO_2 (eluent: 5%-30% MeOH in $CHCl_3$). Evaporation of the solvent followed by high vacuum for 16 h afforded **21** as a white solid (712 mg, 88% yield). MP: 87-90ºC. ^{1}H NMR: 0.88 (t, 11H); 1.17 (s, 10H); 1.26 (bs, 74H); 1.60 (d, 7H); 3.09-4.47 (m, 29H); 7.15 (bs, 1H); 7.67 (bs, 2H); 8.02 (bs, 3H) ppm.

2.23 Preparation of Phospholipid Vesicles and Chloride Release Experiments

1,2-Dioleoyl-*sn*-glycero-3-phosphocholine (DOPC) and 1,2-dioleoyl-*sn*-glycero-3-phosphate (DOPA) were obtained from Avanti Polar Lipids® as 25 mg in 2.5 mL $CHCl_3$ solutions. For each vesicle preparation, a dry film sample of DOPC:DOPA (15 mg, 7:3 w/w) was dissolved in 375 µL Et_2O and then 375 µL internal buffer (600 mM KCl, 10 mM N-2-hydroxyethylpiperazine-*N'*-2-ethanesulfonic acid (HEPES), pH adjusted to 7.00) was added. The mixture was sonicated for 30 s yielding an opalescent suspension. The diethyl ether was removed under low vacuum conditions at 30ºC for 2 hours. The resulting mixed micellar aqueous suspension was filtered through a 200 nm pore-size membrane filter 9 times using a small extruder to obtain a uniform size of vesicles. The filtered suspension was passed through a Sephadex G25 size exclusion column that had been equilibrated with external buffer (400 mM K_2SO_4, 10 mM HEPES, adjusted to pH 7.00) in order to eliminate the extra-vesicular chloride ions. The vesicles were collected and subsequently characterized by using dynamic light scattering. The size of the resulting purified vesicles was confirmed to be ~200 nm. The final lipid concentration was obtained by using a colorimetric determination of the phospholipid-ammonium ferrothiocyanate complex.

The chloride release from liposomes was assayed by using a chloride sensitive electrode (Accumet Chloride Combination Electrode). The electrode was immersed in the vesicle solution

(0.31 mM) and allowed to equilibrate. After 5 minutes an aliquot of the compound solution was added to the vesicle suspension to a concentration of 65 μM. The solution of compounds were prepared usually in a concentration of 9 mM to minimize the amount of 2-propanol and hence its effect on the liposomes. At the end of each experiment the 100 mL of a 2% Triton X-100 solution was added to the vesicle suspension to induce vesicular lysis and to obtain the total chloride concentration. The data collected (DigiData 1322A series interface and Axoscope 9.0 software) were then normalized to this value.

3. RESULTS AND DISCUSSION

3.1 The Heptapeptide SATs

As noted in the introduction, the essential elements of the SAT amphiphiles comprise four modules. These are illustrated in Fig. 1. The twin hydrocarbon tails were designed to function as membrane anchors that mimic the fatty acid chains of phospholipids. [45] The diacid, shown in the Figure as ~$COCH_2YCH_2CO$~ is a linker intended to join the anchor groups with the heptapeptide and to mimic the glyceryl regime of phospholipids. [43] The heptapeptide sequence was initially modeled on the putative selectivity filter of the ClC chloride-transporting protein. [39] The *C*-terminal end of the heptapeptide is esterified with a *n*-heptyl group that prevents carboxyl ionization [46] and serves as a "secondary" membrane anchor.

3.2 Compounds Used

All of the compounds used in the present study are heptapeptides. In previous work, we surveyed the effects of varying the *N*-terminal twin anchor chain, the linker, and the *C*-terminal "secondary" anchor. [41] Likewise, we have examined the effect of changes in the peptide sequence while keeping the other variables constant. For the present study, the *C*-terminal anchor chain was always *n*-heptyl and the peptide always contained seven amino acids in the form $(Aaa)_3Pro(Aaa)_3$. Early work showed that when proline at position 4 was replaced either by leucine or other cyclic amino acids, Cl^- ion release from liposomes was significantly reduced [47].

The compounds studied were typically prepared by reaction of a diamine (the *N*-terminal anchor) with a diacid anhydride to form the anchor and linker modules, $R_2NCOCH_2YCH_2COOH$ in one step. In much of the early work and in the present report, diglycolic acid (Y = O) was the linker of choice. Alternately, thiadiglycolic acid ($HOOCCH_2SCH_2COOH$) anhydride or succinic anhydride (Y is absent) comprised the diacid linker element. A study of linker elements suggested that these three units were among the best to foster Cl^- ion release from liposomes. [48] The diamines were di-*n*-hexylamine, di-*n*-dodecylamine, or di-*n*-octadecylamine. Previous studies showed that shorter anchor chains afforded greater Cl^- ion release from liposomes, but at a cost of anion *vs*. cation selectivity [49].

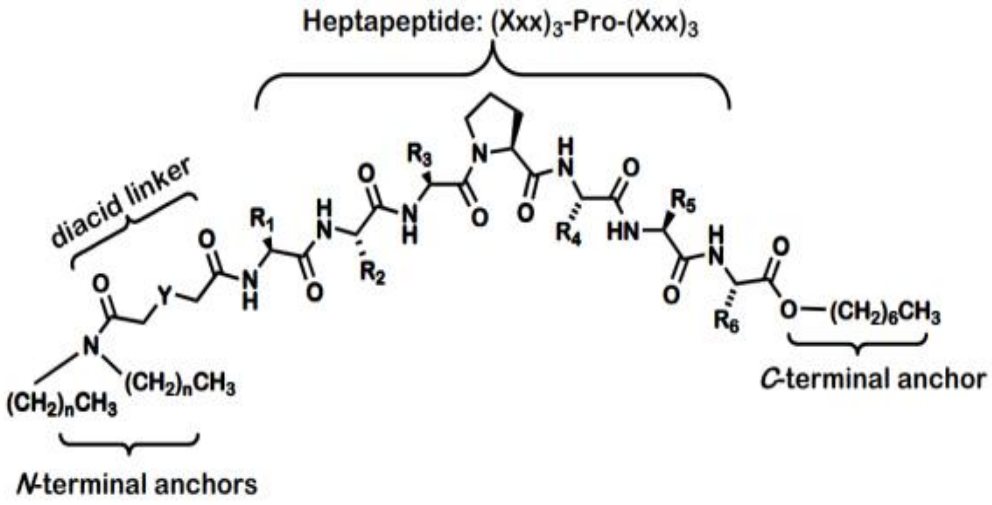

Fig. 1. General structure for synthetic anion transporter (SAT) amphiphiles

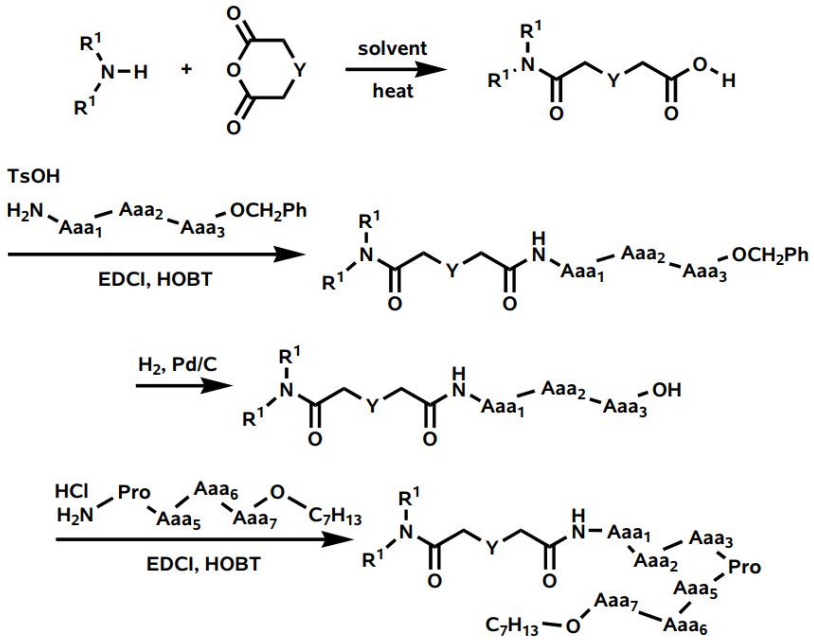

Scheme 1. Synthesis of SATs (1-21). The abbreviations A_n and Aaa_n represent amino acids. Y may represent O, S, or be absent

The assembly of the SATs reported herein was accomplished in a straightforward and modular manner. As noted above, the incipient linker was a diacid converted into its anhydride. This was treated with a diamine to form the $R_2NCOCH_2YCH_2COOH$ module. Commercially available triglycine or trialanine was coupled to proline using a standard HBTU protocol. Triglycine or other tripeptide was esterified with *n*-heptanol and the two fragments coupled to give $R_2NCOCH_2YCH_2CON(Aaa)_7OC_7H_{15}$. Where peptide protection was required, standard methods were employed. [50] The synthesis is illustrated in Scheme 1. The product SATs are shown in Table 1 with reference to Scheme 1.

3.3 Anion Transport

Anion release from liposomes was studied in various ways. The anion most commonly assessed was Cl^-, which was detected as egress from DOPC:DOPA (7:3) liposomes (0.31 mM) mediated by SATs (65 μM at pH 7), using a Cl^--selective electrode. Alternately, the chloride selective dye lucigenin was used to detect Cl^- transport. [38] Fluorescein transport was studied as well. Fluorescein is often used as a surrogate for Cl^- because it can readily be detected at low concentrations.

An example of how the anchor chain (R) length in $R_2NCOCH_2YCH_2CO\text{-}G_3PG_3\text{-}OCH_2Ph$ affects carboxyfluorescein (CF) release is shown in Fig. 2. This is a convenient experiment because CF within vesicles is self-quenched. The highly fluorescent dye that emerges is readily detectable by fluorimetry. The di-*n*-alkyl chains that comprise the *N*-terminal anchors for the SAT ranged in length in this experiment from *n*-octyl to *n*-octadecyl. The experiment was arbitrarily terminated at 300 s, by which time the shortest chain compounds had released all of the dye. The 100% release value was determined by using Triton X-100 detergent to lyse the vesicles. The total dye was set to a value of 100% and compared to the amount released prior to lysis. Release is then expressed as a percentage. Fig. 2 shows the length dependence of the "R" *N*-terminal anchor chains in $R_2NCOCH_2OCH_2COG_3PG_3OCH_2Ph$. Although the graph shows CF release, generally similar behavior has been observed for Cl^- release from liposomes [38] when using Cl^--selective electrodes or lucigenin [51].

It should be noted that the compounds recorded in Table 1 and the compounds used in the CF release-rate study shown in Fig. 2 differ from 1-21 in the *C*-terminal anchor. A study of the effect of variations in the *C*- and *N*-terminal chains *N*-

terminal chains (R^1) and C-terminal (R^2) anchors in $R^1{}_2NCOCH_2OCH_2COG_3PG_3OR^2$ has previously been reported. [52] The *C*-terminal anchors (R^2) included O-Et, O-*n*-heptyl, O-benzyl, O-methylenecyclohexyl, and O-*n*-octadecyl. The two most favorable for ion transport were O-*n*-heptyl and O-benzyl. Similar, although not identical, behavior was observed for these two seven-carbon C-termini. Thus, the comparison of Cl^- release data shown in Table 1 and the CF release data plotted in Fig. 2 are relevant to each other and to the results presented here.

Table 1. Structures of Compounds 1-21[a]

No.	Twin *N*-anchors	Linker[b]	Peptide	% Cl^- release[c]
1	*n*-C_6H_{13}	~$COCH_2CH_2CO$~	GGGPGGG	60
2	*n*-$C_{10}H_{21}$	~$COCH_2CH_2CO$~	GGGPGGG	ND[d]
3	*n*-$C_{12}H_{25}$	~$COCH_2CH_2CO$~	GGGPGGG	ND
4	*n*-$C_{18}H_{37}$	~$COCH_2CH_2CO$~	GGGPGGG	70
5	*n*-C_6H_{13}	~$COCH_2$**O**CH_2CO~	GGGPGGG	ND
6	*n*-$C_{18}H_{37}$	~$COCH_2$**O**CH_2CO~	GGGPGGG	60
7	*n*-$C_{12}H_{25}$	~$COCH_2CH_2CO$~	AAAPGGG	11
8	*n*-$C_{18}H_{37}$	~$COCH_2CH_2CO$~	AAAPGGG	11
9	*n*-$C_{12}H_{25}$	~$COCH_2$**O**CH_2CO~	AAAPGGG	28
10	*n*-$C_{18}H_{37}$	~$COCH_2$**O**CH_2CO~	AAAPGGG	20
11	*n*-$C_{18}H_{37}$	~$COCH_2$**S**CH_2CO~	AAAPGGG	20
12	*n*-$C_{12}H_{25}$	~$COCH_2CH_2CO$~	GGGPSGS	13
13	*n*-$C_{18}H_{37}$	~$COCH_2CH_2CO$~	GGGPSGS	10
14	*n*-$C_{18}H_{37}$	~$COCH_2$**O**CH_2CO~	GGGPSGS	13
15	*n*-$C_{12}H_{25}$	~$COCH_2CH_2CO$~	GGGPS(*t*-Bu)GS(*t*-Bu)	28
16	*n*-$C_{18}H_{37}$	~$COCH_2CH_2CO$~	GGGPS(*t*-Bu)GS(*t*-Bu)	24
17	*n*-$C_{12}H_{25}$	~$COCH_2$**O**CH_2CO~	GGGPS(*t*-Bu)GS(*t*-Bu)	30
18	*n*-$C_{18}H_{37}$	~$COCH_2$**O**CH_2CO~	GGGPS(*t*-Bu)GS(*t*-Bu)	27
19	*n*-$C_{12}H_{25}$	~$COCH_2CH_2CO$~	GGGPGS(*t*-Bu)G	ND
20	*n*-$C_{18}H_{37}$	~$COCH_2CH_2CO$~	GGGPGS(*t*-Bu)G	ND
21	*n*-$C_{18}H_{37}$	~$COCH_2$**O**CH_2CO~	GGGPGS(*t*-Bu)G	ND

a. All compounds have a C-terminal n-heptyl anchor (see Fig. 1). b. Linker heteroatoms are in bold type for clarity. c. Chloride release from DOPC:DOPA (7:3) liposomes mediated by SATs (see Experimental section for details). d. ND means not determined under these conditions

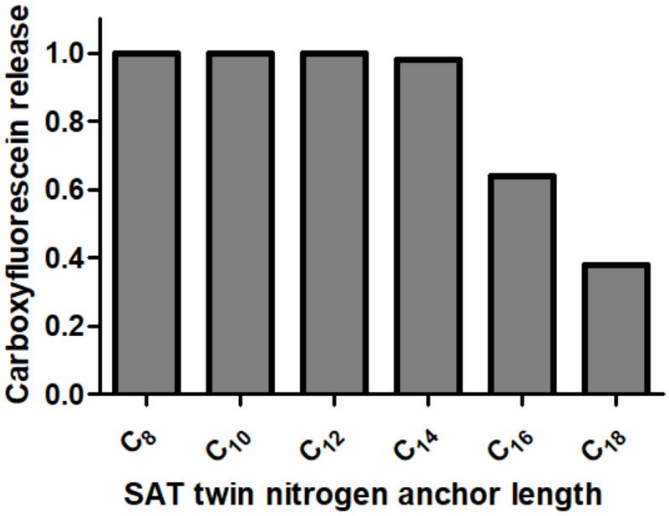

Fig. 2. Carboxyfluorescein release from DOPC:DOPA (7:3) liposomes (0.31 mM) mediated by $R_2NCOCH_2OCH_2COG_3PG_3OCH_2Ph$ (65 μM at pH 7) in which the twin *N*-terminal anchor chains (R_2) range from *n*-octyl to *n*-octadecyl. The values reflect release at 300 s

3.4 Experimental Plant Studies

Arabidopsis thaliana is the best known and most widely studied experimental plant. The most commonly used strain, "Col-0," for which the entire genome is known, was used in the present study. [29] The growth medium was sterilized agar containing plant nutrient plus sucrose or "PNS" as described in the experimental section. Approximately 20 seeds were germinated on each plate and each experiment was conducted in at least triplicate. This resulted in each data point representing 60 or more observations. Plants were allowed to grow under continuous white light for 11 days, at which time the root properties were determined by visual analysis using a dissecting microscope.

The data reported are the primary root length, measured in millimeters, and the number of lateral roots, assessed visually. The *lateral root density* is an arbitrarily defined, unit-less value obtained by dividing the number of lateral roots by the length of the primary root in millimeters. Thus, if the average length for 60 plants of the primary root is 35 mm and the average number of lateral roots counted is 5.25, then the lateral root density would be (5.25/35 =) 0.15. Similarly, if the average primary root length is 45 mm and the average number of lateral roots is 6.75, the lateral root density would be (6.75/45 =) 0.15. The numbers shown were deliberately chosen to illustrate the possibility of accidental coincidence.

3.4.1 Controls

Approximately 60 plants were grown on PNS media (no additives). Root lengths and the number of lateral roots were recorded for each plant. The data points were averaged to obtain the following baseline values: primary root length = 40.4 ± 3.8 mm and number of lateral roots = 6.1 ± 0.8, respectively. The experimentally determined lateral root density determined as the control value based on these observations is (6.1/40.6 =) 0.15.

The test compounds were added to the growth medium using an amount of DMSO equal to 0.2% of the final solution volume. A control (60 plants) for DMSO at this concentration[53] showed no effect on germination, growth, or on root morphology compared to the PNS control absent DMSO (data not shown). This step was critical as DMSO is known to affect membrane permeability[54] and, as a consequence, biological activity if the concentration is sufficiently high.[55] Each SAT was added to a concentration of 50 μM in the PNS/agar growth medium. This value was chosen so that the effect of SATs, if any, on *A. thaliana* could be compared with results previously obtained with hydraphiles.[6]

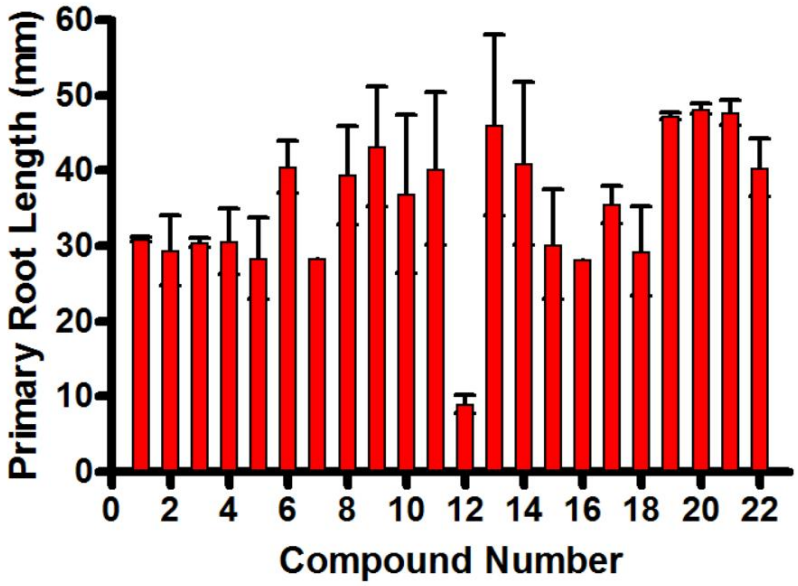

Fig. 3. Plot of calculated lateral root density for compounds 1-21. The data for 22 (PNS) and 23 (2,4-D) are controls (see text)

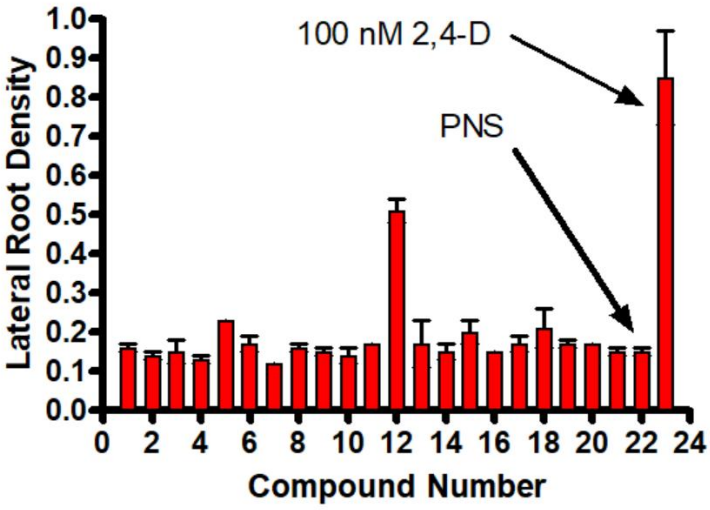

Fig. 4. Plot of primary root length (in mm) for compounds 1-21. The data for 22 are for the control plants (see text)

2,4-Dichlorophenoxyacetic acid (2,4-D) is a well-known broad leaf herbicide. It mimics the action of the natural growth hormone indoleacetic acid. 2,4-D acts by overstimulating growth with an ultimately toxic effect. It was used as a positive control in the present study. Based on the extreme difference in structure between 2,4-D and SATs, any effect of the latter seems likely to occur by a different mechanism. 2,4-D was present in the PNS medium at a concentration of 100 nM and plants were grown as noted above. This synthetic hormone significantly decreased both primary root length and lateral root number to 3.9 ± 0.6 mm and 3.4 ± 0.6, respectively. The calculated lateral root density in this case is (3.4/3.9=) 0.85 (control = 0.15).

The results obtained for the 21 compounds included in this study are shown in the graph of Fig. 3. The SATs are identified by number (*see* Table 1). The designation **22** refers to the plant growth controls (average of ~60 plants). The designation **23** refers to (~60) plants grown under the same conditions as controls with the toxin (2,4-D) added to the growth media at the 100 nM level.

A similar plot is shown in Fig. 4, in which the ordinate is primary root length. In this case, the effect of 2,4-D is not included, but position 22 again corresponds to control. The correspondence in shortened primary root length and higher lateral root density for compound **12** is apparent. Other points deserve note and are discussed below in terms of heptapeptide sequence.

3.4.2 SATs having a $(Gly)_3Pro(Gly)_3$ heptapeptide sequence

The SAT compounds that we have studied most extensively in the past have a $(Gly)_3Pro(Gly)_3$ heptapeptide sequence. [37] These compounds were designed to be chloride ion transporters and planar bilayer conductance data obtained by others confirmed this function. [56] Compounds **1**-**6** all have the G_3PG_3 peptide sequence and *C*-terminal *n*-heptyl esters, but differ both in the *N*-terminal anchor and linker chains. The primary root length and the number of lateral roots for **6** is within experimental error of the PNS control. The average primary root length for **1**-**5** is 30 mm, which compares with 40.4 mm for the PNS control. there is thus a mild growth retardation, which we infer is a modest toxic effect.

The shortest average root length for *A. thaliana* in the **1**-**5** series is exhibited by **5**, $(C_6)_2NCOCH_2OCH_2COG_3PG_3OC_7$. It is 28.4 ± 5.4 mm. This is significantly shorter than the control value of 40 mm. The average number of lateral roots observed for **1**-**5** is 4.7. This compares to a control of 6.1 ± 0.8, a difference of nearly 30%. The calculated lateral root density for **1**-**5** is (4.7/28.4 =) 0.165. This appears to differ little from the control value of 0.15, but this is a consequence of fewer lateral roots being divided by a shorter primary root. Thus, the

behavior of **1**-**5** is statistically, if not remarkably different from control, or attributable to a specific cause. This is especially apparent for **5**, for which the lateral root density is (6.6/28.4 =) 0.23. Like **5**, **1** has *n*-hexyl side chains. Its structure is $(C_6)_2NCOCH_2CH_2COG_3PG_3OC_7$, and its lateral root density is 0.16. Compound **6** in this family (C_{18} anchors, diglycolic) fits within control parameters. We conclude that the biological effect is greater for succinyl spacers and/or shorter anchor chains. This comports with the results of a study using planar bilayer conductance showing that succinyl linkers generally foster greater conductance than do diglycoyl linkers. We infer that the Cl^- imbalance affects root morphology.

3.4.3 SATs having the $(Ala)_3Pro(Gly)_3$ heptapeptide sequence

The heptapeptide sequence in compounds **7**-**11** is $(Ala)_3Pro(Gly)_3$. The peptide sequence in this group of compounds was of interest because earlier studies showed that the strongest interactions with the peptide involved hydrogen bond donation to Cl^- from to ^{5}Gly and ^{7}Gly. [57] No previous study explored variations in the peptide sequence on the *N*-terminal side of proline. Compounds **7** and **8** have succinyl linkers and **9** and **10** are linked by diglycolic acid diamide. A different linker is present in **11**, which has the structure $(C_{18})_2NCOCH_2\mathbf{S}CH_2CO\text{-}A_3PG_3\text{-}OC_7$. The linker here is thiodiglycolic acid (Fig. 1, Y = S). In short, no significant deviation from control was observed with **8**-**11** despite variations in linker and anchor chain lengths. Compound **6** may be compared directly to **10**. Their structures (C_{18} anchors, diglycoyl linkers) are identical except for the G_3PG_3 (**6**) *vs*. A_3PG_3 (**10**) peptide sequences. Neither compound differs significantly from the control in its biological effect on *A. thaliana*. As noted above, binding favored interactions on the C-terminal side of proline. Thus, the $G_3 \rightarrow A_3$ alteration was not expected to show a significant difference in root development.

Compound **7**, however, which has the structure $(C_{12})_2NCOCH_2CH_2CO\text{-}A_3PG_3\text{-}OC_7$, showed reduced primary root length (28.4 mm) comparable to that observed for **1**-**5**, but an even smaller number of lateral roots (3.4). SATs **7** and **8** are identical except for the *N*-terminal anchor chains, which are *n*-dodecyl in **7** and *n*-octadecyl in **8**. In an earlier study, we found that Cl^- transport was greater for $(C_n)_2NCOCH_2OCH_2CO\text{-}GGGPGGG\text{-}OCH_2Ph$ when C_n was *n*-dodecyl compared to *n*-octadecyl. It was concluded that the octadecyl compound was more selective, but less efficient, and that the dodecyl compound likely was transporting both Na^+ and Cl^- ions. [58] If a similar effect on ion transport occurs in the case of **7**, it would explain the difference between the activities of **7** and **8**. Of course, this cannot be the only effect as the anchor chain difference is present in **9** and **10**, which are otherwise comparable, and their root profiles are similar to each other and to controls.

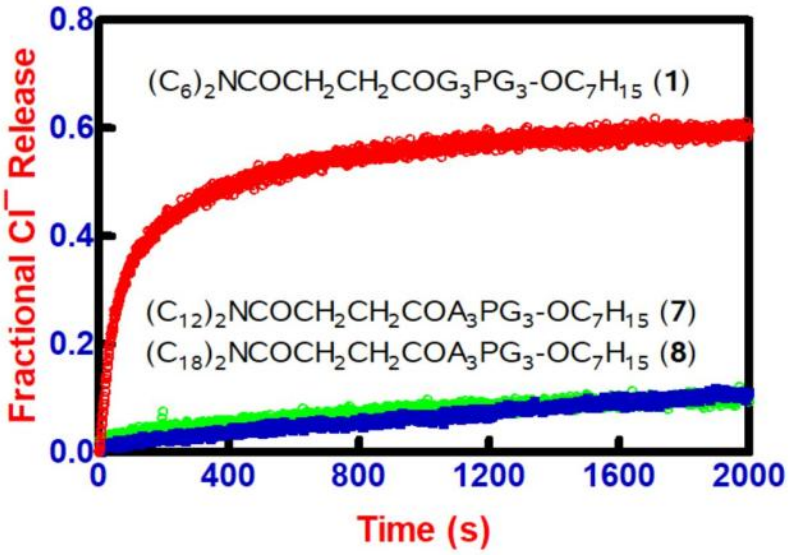

Fig. 5. Fractional release of Cl^- from DOPC:DOPA (7:3) liposomes (0.31 mM) mediated by succinic acid linked SATs 1, 7, and 8

We also note that **10** and **11** (C_{18} anchors, A_3PG_3 peptide) behave in a fashion similar to each other and to controls despite the difference in diglycolic (**10**) and thiadiglycolic (**11**) linkers. Taken together, some statistically significant differences in plant response to all glycine or alanine-glycine heptapeptides are observed, but these effects were minor.

3.4.4 SATs containing one or more serine residues in the heptapeptide sequence

Table 2, which shows details for compounds **12**-**21**, reveals a number of effects manifested by the presence of serine in the heptapeptide chain. The serines occur on the *C*-terminal side of proline and the hydroxyl group(s) are either protected (*t*-butylated) or free.

Ten of the compounds reported here incorporate one or more serines into the heptapeptide sequence. The lateral root densities and the primary root lengths for **1**-**21** are plotted in Figs.3 and 4, respectively (above). Table 2 shows the compounds in three groups and includes the numerical information upon which the graph of Fig. 4 is based. The peptides were prepared by coupling a G_3P fragment to either an SGS or GSG segment in which the serine hydroxyl groups were protected as the *t*-butyl ethers. As a result, we obtained **12**-**14** with free hydroxyl groups and **15**-**21** in their protected forms.

The simplest compounds in this group of three are **19**-**21**, in which the single serine in the G_3PGSG sequence is protected by *t*-butyl. Compounds **20** and **21** differ in having succinyl and diglycoyl linkers, but are otherwise identical. Compound **19** has the succinyl linker chain of **20**, but has twin dodecyl anchor chains rather than the octadecyl chains present in both **20** and **21**. The average primary root length measured for **19**-**21** was 47.7 mm and the variation in this value was small. The length is significantly longer (~20%) than the control value of 40.4 mm. Likewise, the average number of lateral roots (7.6) is about 25% greater than control. Since the lateral root density is higher and the primary root length is longer, the calculated lateral root density is similar to the control value. Overall, it appears that this group of SATs stimulates the growth of *A. thaliana* without significantly altering its growth characteristics of the whole plant. The results observed for the *bis*(serinyl) di-*t*-buyl ethers in **15**-**18** approximately parallel those observed for **1**-**5** and seem to exhibit the opposite of the effect observed for **19**-**21**.

3.4.5 Comparisons of heptapeptide sequence effects

Two sets of compounds have identical *N*- and *C*-terminal anchor chains and succinyl linkers. They are **3**, **7**, **12**, **15**, and **19** *vs*. **4**, **8**, **13**, **16**, and **20**. Direct comparisons can be made between the following pairs: **3,4**; **7,8**; **12,13**; **15,16**; and **19,20**. These pairs have C_{12} and C_{18} *N*-terminal anchor chains, respectively, but otherwise are identical. The pairs differ from one another in the heptapeptide sequences. Fig. 6 shows the effect of peptide sequence on primary root length (left) and lateral root density (right). Plants grown under control conditions have a primary root length of 40.4 mm, as indicated in the graph by the dashed line.

Table 2. Root Morphology Data for 12-21

Compound Number (50 µM)	Primary root length (mm)	Number of lateral roots	Lateral root density
PNS (±0.2% DMSO)	40.4 ± 3.8	6.1 ± 0.8	0.15 ± 0.01
2,4-D (100 nM)	3.9 ± 0.6	3.4 ± 0.6	0.85 ± 0.12
GGGPSGS			
Compound **12**	9.0 ± 1.2	4.5 ± 0.4	0.51 ± 0.03
Compound **13**	46.0 ± 12.0	8.7 ± 4.9	0.17 ± 0.06
Compound **14**	40.9 ± 10.8	6.2 ± 2.4	0.15 ± 0.02
GGGPS(tBu)GS(tBu)			
Compound **15**	30.2 ± 7.3	5.8 ± 0.7	0.20 ± 0.03
Compound **16**	28.3	5.9	0.15
Compound **17**	35.5 ± 2.5	5.9 ± 0.2	0.17 ± 0.02
Compound **18**	29.3 ± 5.9	5.2 ± 0.3	0.21 ± 0.05
GGGPGS(tBu)G			
Compound **19**	47.3 ± 0.5	7.9 ± 0.5	0.17 ± 0.01
Compound **20**	48.2 ± 0.7	8.2	0.17
Compound **21**	47.7 ± 1.7	6.8	0.15 ± 0.01

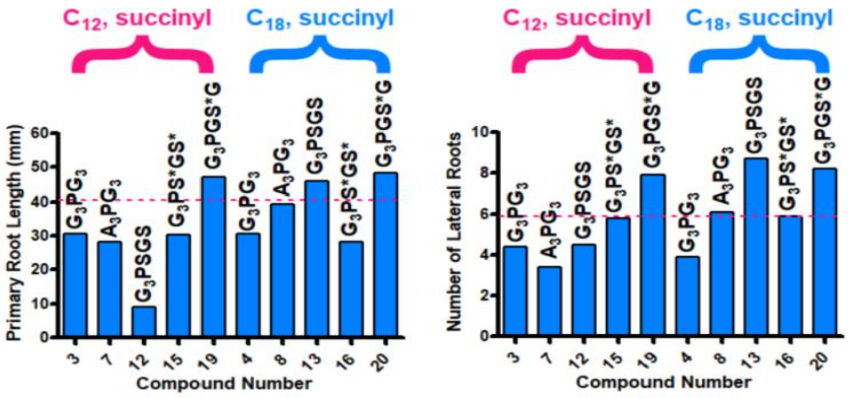

Fig. 6. Left panel: Comparison of primary root lengths in pairs of compounds having C_{12} and C_{18} *N*-terminal anchors and succinyl linkers. The pairs have the following heptapeptide sequences: 3,4 (GGGPGGG); 7,8 (AAAPGGG); 12,13 (GGGPSGS); 15,16; [GGGPS(*t*-Bu)GS(*t*-Bu)];and 19,20 [GGGPGS(*t*-Bu)G]. The dashed line indicates the primary root length of the controls. Right panel: Comparison of the number of lateral roots observed in pairs of compounds having C_{12} and C_{18} *N*-terminal anchors and succinyl linkers. The dashed line indicates the lateral root number of the controls. The symbol "S*" indicates a serine having a *t*-butylated hydroxyl group. Error bars have been omitted for clarity

Three compounds show primary root lengths significantly greater than controls. They are **13** (C_{18}, GGGPSGS), **19** and **20** [C_{12} and C_{18} GGGPGS(*t*-Bu)G]. All three contain serine and all three stimulate primary root length to about the same extent (see Table 2). The C_{18} SAT incorporating the AAAPGGG peptide (**8**) shows no effect on primary root length. Compounds **3**, **4**, **7**, **15**, and **16** all affect *A. thaliana* growth by diminishing primary root length. That the **3**,**4** and **15**,**16** pairs behave the same suggests that it is the peptide sequence that is important rather than the *N*-terminal chain length. However, compound **7** reduces primary root length while its partner, **8**, shows no effect, suggesting that the peptide sequence alone cannot account for the difference. It is noted that this difference is relatively small when the error bars (not shown on graph) are taken into account.

The most striking results are observed with the **12**,**13** pair. In both cases, the heptapeptide sequence is GGGPSGS. The *N*-terminal anchor chains are C_{12} in **12** and C_{18} in **13**. The former shows a dramatic reduction in primary root length and the latter an increase outside of experimental error relative to control. In a previous study, it was found that the amide hydrogens of amino acids ^{5}G and ^{7}G were the key Cl^--binding donors when studied by NMR in a micellar matrix. [57] At present, we have no direct evidence that Cl^- – or any ion – binding is critical to the effect these compounds have on plants. Notwithstanding, the difference in effect on *A. thaliana* by **12** and **13** is dramatic and striking.

The results shown in Fig. 6 parallel those of Fig. 2. They show the effect of the same compounds on the number of lateral roots observed when administered to *A. thaliana*. As with primary root length, compounds **13**, **19**, and **20** show enhancements relative to controls. As with primary root length, **8** shows no effect on lateral root number. In contrast, compounds **3**, **4**, **15**, and **16** showed similar, reduced primary root length, but the number of lateral roots is unaltered by the presence of **15** and **16**. The lateral root number is diminished by the presence of **4** and **7** by an approximately equal amount and **12** does not show such a dramatic effect as is apparent in primary root length.

3.4.6 The activity of the GGGPSGS compounds, 12 and 13

The most striking observation made in this study is the effect of **12** and **13** on *A. thaliana*. Their structures are $(C_{12\ or\ 18})_2NCOCH_2CH_2CO$-$G_3PSGS$-$OC_7$. Four observations are remarkable about the SAT's biological activity. First, these compounds dramatically reduce the primary root length of the test plants. Second, the number of lateral roots are statistically below control, but not dramatically different from other, less active, heptapeptides. Third, the potent biological activity of **12** is lost by protecting the two serine hydroxyl groups. Fourth, the longer *N*-terminal anchor chains essentially void the effects

observed in **12**. Indeed, longer-chained **13** shows a slightly longer primary root and significantly more lateral roots than its shorter-chained congener.

The NMR study noted above showed that the glycines in the G_3PG_3 peptide's 5 and 7 positions were most intimately involved with Cl^-. The hydrogen atoms were not located in this NMR structure, but the conformation strongly suggested >N—H hydrogen bond interactions. These may persist in **12** and be augmented by the two serine hydroxyls that are in the 5 and 7 positions. This explanation would lead one to conclude that **12** and **13** would behave similarly. Although their ability to release Cl^- from phospholipid liposomes is similar (**12**: 13%; **13**: 10%), both exhibit poor Cl^- transport. Compound **4**, in contrast, is identical to **13** except its heptapeptide is G_3PG_3 and its Cl^- release in 300 s is 70%.

Earlier studies showed that when otherwise identical SATs were compared, the compound with the C_{12} anchors showed greater transport efficacy and poorer selectivity than the analog with C_{18} anchors. In addition, selectivity for Cl^- was lost by the C_{12} compound suggesting that Na^+ and Cl^- were both being transported. The presence of cations and anions within the channel could account for a difference in biological activity, but the loss of selectivity observed in that study was accompanied by higher overall transport that is not observed here. It remains unclear why several of the serine-containing SATs show both longer primary roots and an increased number of lateral roots.

3.4.7 Comparison of SAT antibacterial activity with the action on *A. thaliana*

Compounds **1**-**21** were studied to determine if they exhibited toxicity to the K-12 strain of *Escherichia coli*. In these experiments, the minimum inhibitory concentration was determined by using the Clinical and Laboratory Standards Institute M07-A9 protocol. [59] None of the SATs reported here showed any toxicity to *E. coli* at concentrations below 256 μM (data not shown). Of course, *A. thaliana* and *E. coli* are classified in different biological domains so this difference in activity may be expected. Notwithstanding, our previous observation that hydraphile pore-formers, which transport cations rather than anions, are toxic to bacteria and show a significant effect on *A. thaliana* led us to anticipate a different outcome.

3.4.8 Comparison of SATs with Lariat Ethers and Hydraphiles

Previous work evaluated the ability of lariat ethers[10] or hydraphiles[6] to affect root morphology in *A. thaliana*. Hydraphiles showed a general correlation between cation transport efficacy and increased lateral root development. Several of the lariat ethers tested were known transporters, but were found to show clear evidence (planar bilayer conductance) for pore formation. It was inferred in both cases that ion transport was affected leading to root alterations by a mechanism different from that controlled by auxins. The SATs were designed to conduct Cl^- and considerable evidence confirms that. In terms of activity in the development of *A. thaliana*, we conclude that the compounds that exhibit the greatest effect are those that can also transport cations (short *N*-anchors) or interact effectively with endogenous cations (serine containing peptides).

4. CONCLUSIONS

The SATs are Cl^--selective pore-formers that generally have little effect on the root morphology of *A. thaliana*. The exceptions are notable, however. These fall into three categories. First, the G_3PG_3 peptides all inhibit both primary root growth and the number of lateral roots that form. The fact that root length is compromised without compensatory lateral root development suggests a toxic effect. Second, the placement of two serines having pendant hydroxyl groups on the C-terminal side of proline seems ideal to interact with cations as well as anions and exhibits the most dramatic effect on root development. The third observation is that when the serine hydroxyl groups are protected, plant growth is stimulated. We conclude that the SATs are generally biologically active in this context, but that the greatest effects are apparent when interactions with cations, rather than anions, are possible.

ACKNOWLEDGEMENTS

We gratefully acknowledge support of this work by the National Science Foundation under grants CHE 1307324, CHE 1710549 and by the University of Missouri-St. Louis.

COMPETING INTERESTS

A patent application has been submitted, the rights to which are held by the Curators of the University of Missouri. Otherwise, no competing interests exist.

REFERENCES

1. Gokel GW, Negin S. Synthetic membrane active amphiphiles, Adv. Drug. Deliv. Rev. 2012;64(9):784-96.
2. Gokel GW, Negin S. Synthetic Ion Channels: From Pores to Biological Applications Acc. Chem. Res. 2013;46(12):2824–2833.
3. Ugras HI, Cakir U, Azizoglu A, Kilic T, Erk C. Experimental, Theoretical and Biological Activity Study on the Acyl-Substituted Benzo-18-crown-6, Dibenzo-18-crown-6 and Dibenzo-24-crown-8 J. Incl. Phenom. Macrocyclic Chem. 2006;55:159-165.
4. Huang ST, Kuo HS, Hsiao CL, Lin YL. Efficient synthesis of 'redox-switched' naphtho-quinone thiol-crown ethers and their biological activity evaluation Bioorg. Med. Chem. 2002;10:1947-52.
5. Sadeghian A, Seyedi SM, Sadeghian H, Hazrathoseyni A, Sadeghian M. Synthesis, biological evaluation and QSAR studies of some new thioether-ester crown ethers, J. Sulfur Chem. 2007;28:597-605.
6. Eshghi H, Rahimizadeh M, Zokaei M, Eshghi S, Eshghi S, Faghihi Z, Tabasi E, Kihanyan M. Synthesis and antimicrobial activity of some new macrocyclic bis-sulfonamide and disulfides, Eur. J. Chem. 2011;2:47-50.
7. Zaim O, Aghatabay NM, Gurbuz MU, Baydar C, Dulger B. Synthesis, structural aspects, antimicrobial activity and ion transport investigation of five new [1+1] condensed cycloheterophane peptides, J. Incl. Phenom. Macrocycl. Chem. 2014;78: 151-159.
8. Le TA, Truong HH, Thi TPN, Thi ND, To HT, Thia, HP; Soldatenkov, AT., Synthesis and biological activity of (gamma-arylpyri-dino)-dibenzoaza-14-crown-4 ethers, Mendeleev Commun. 2015;25:224-225.
9. Gumus A, Karadeniz S, Ugras HI, Bulut M, Cakir U, Gorend AC. Synthesis, Complexation, and Biological Activity Studies of 4-Aminomethyl-7,8-dihydroxy Coumarines and Their Crown Ether Derivatives, J. Heterocyclic Chem. 2010;47: 1127-1133.
10. Ozay H, Yildiz M, Unver H, Dulger B. Synthesis, spectral studies, antimicrobial activity and crystal structures of phosphaza-lariat ethers, Asian J. Chem. 2011;23:2430-2436.
11. Kiraz A, Yildiz M, Dulger B. Synthesis and characterization of crown ethers, Asian J. Chem. 2009;21:4495-4507. (j) Konup LA, Konup IP, Sklyar VE, Kosenko KN, Gorodnyuk VP, Fedorova GV, Nazarov EI, Kotlyar SA. Antimicrobial activity of aliphatic and aromatic crown-ethers, Khimiko-farmatsevticheskii Zhurnal. 1989;23:578-583.
12. Devinsky F, Lacko I, Inkova M. Preparation of antimicrobially active amphiphilic azacrownethers of amine oxide and quaternary ammonium salt type, Die Pharmazie. 1990;45:140.
13. Devinsky F, Devinsky H, Czechoslovakia Patent 274 873 issued; 1991.
14. Ugras HI, Cakir U, Azizoglu A, Kilic T, Erk C. Experimental, Theoretical and Biological Activity Study on the Acyl-Substituted Benzo-18-crown-6, Dibenzo-18-crown-6 and Dibenzo-24-crown-8, J. Incl. Phenom. Macrocyclic Chem. 2006;55:159-165.
15. Kato N. Antibacterial action of alkyl-substituted crown ethers, Kenkyu Kiyo - Konan Joshi Daigaku. 1985;585-96. (o) Tso W-W; Fung, W-P, Tso M-YW. Variability of crown ether toxicity, J. Inorg. Biochem. 1981;14:237-244.
16. Plotnikova EK, Golovenko NY, Zin'kovskii VG, Luk'yanenko NG, Zhuk OV, Basok SS. Transport and metabolism of a membrane-active complexon in mice, Voprosy Meditsinskoi Khimii.1987;33:62-66.
17. Timofeeva SE, Voronina TA, Karaseva TL, Golovenko NY, Garibova TL, Luk'yanenko NG. Psychotropic effects of some derivatives of N-crown ethers Farmakologiya i Toksikologiya (Moscow). 1986;49:13-15.
18. Van'kin GI, Lukoyanov NV, Galenko TG, Raevskii OA. Pharmacologic activity of crown ethers, Khimiko-Farmatsevti-cheskii Zhurnal 1988;22:962-5.
19. Lukoyanov NV, Van'kin GI, Sapegin AM, Raevskii OA. Physicochemical modeling of structure-activity relations. Macrocyclic anticonvuls-ants, Khimiko-farmatsevticheskii Zhurnal.1990;24:48-51.
20. Adamovich SN, Mirskova AN, Mirskov RG, Perminova OM, Chipanina NN, Aksamentova TN, Voronkov MG. New Quaternary Ammonium Salts and Metal Complexes of Organylheteroacetic Acids with Diaza-18-crown-6 Ether, Russ. J. Gen. Chem. 2010;80:1007-1010.

21. Kralj M, Majerski K, Ramljak S, Marjanovic M. United States Patent 8,389,505, Issued; 2013.
22. Harris EJ, Zaba B, Truter MR, Parsons DG, Wingfield JN. Specificities of cation permeabilities induced by some crown ethers in mitochondria, Arch. Biochem. Biophys. 1977;182:311-320.
23. Huang D, Wang D, Fu T, Que R, Zhang J, Huang L, Ou H, Zhang Z. Effects of crown ethers on the K+ and Na+ transport of plant roots (1) Effect of benzo-15-crown-5 on the K and Na transport of wheat roots, J. Nanjing Univ. (Nat. Sci.). 1980;33-44.
24. Pemadasa MA. Effects of benzo-18-crown-6 on abaxial and adaxial stomatal opening and its antagonism with abscisic acid, New Phytol. 1983;93:13-24.
25. Macklon AES, Sim A, Parsons DG, Truter MR, Wingfield JN. Effects of some cyclic 'crown' polyethers on potassium uptake, efflux and transport in excised root segments and whole seedlings Ann. Bot. 1983;52:345-356.
26. Huang Z, Yu Z, Shu J. The progress in the study on saturated urushiol crown ethers, Organic Chemistry. 1985;6:497-502.
27. Yuan W, Huang Z, Ruifeng H. Effects of crown ether on some physiological properties and economic characteristics of spikes of wheat and panicles of rice, Wuhan Univ. J. Nat. Sci. 1996;1:259-262.
28. Patel MB, Stavri A, Curvey NS, Gokel GW. Hydraphile synthetic ion channels alter root architecture in Arabidopsis thaliana, Chem. Commun. 2014;50:11562-11564.
29. *A. thaliana* Col 0 was obtained from The Arabidopsis Biological Resource Center (ABRC)
Available: https://abrc.osu.edu
30. Patel MB, Negin S, Stavri A, Gokel GW. Supramolecular Cation Transporters Alter Root Morphology in the Arabidopsis Thaliana Plant, Inorganica Chimica Acta, 2017;468:183-191.
31. Gao K, Chen F, Yuan L, Zhang F, Mi G. A comprehensive analysis of root morphological changes and nitrogen allocation in maize in response to low nitrogen stress. Plant Cell Environ. 2015;38 (4):740-750.
32. Fan J-W, Du Y-L, Turner NC, Wang B-R, Fang Y, Xi Y, Guo X-R, Li F-M. Changes in root morphology and physiology to limited phosphorus and moisture in a locally-selected cultivar and an introduced cultivar of Medicago sativa L. growing in alkaline soil. Plant Soil. 2015;392:215-226.
33. Bernardy K, Farias JG, Dorneles AOS, Pereira AS, Schorr MRW, Thewes FR, Londero JEL, Nicoloso FT. Changes in root morphology and dry matter production in Pfaffia glomerata (Spreng.) Pedersen accessions in response to excessive zinc. Rev. Bras. Pl. Med., Campinas. 2016;18(2, Supl. 1):613-620.
34. Marastoni L, Sandri M, Pii Y, Valentinuzzi F, Cesco S, Mimmo T. Morphological Root Responses and Molecular Regulation of Cation Transporters Are Differently Affected by Copper Toxicity and Cropping System Depending on the Grapevine Rootstock Genotype. Front. Plant. Sci. 2019;10: Article 946.
35. Belatus EL. Morphological Features, Cation Exchange Capacity, and Osmotic Pressure for Different Banana Root Segments. Middle East J. Agriculture. 2018;7:21-26.
36. Strohm AK, Vaughn LM, Masson PM. Natural variation in the expression of ORGANIC CATION TRANSPORTER 1 affects root length responses to cadaverine in Arabidopsis. J. Exp. Botany 2015;66(3): 853-862.
37. Gokel GW, Daschbach MM. Synthetic Amphiphilic Peptides that Self-assemble to Membrane-active Anion Transporters, in Bianchi A; Bowman-James K, Garcia-España E, Supramolecular Chemistry of Anions; 2nd Edition, Wiley-VCH: New York. 2012;45-62.
38. Riccardo Ferdani R, Li R, Pajewski R, Pajewska J, Winter RK, Gokel GW. Transport of chloride and carboxy-fluorescein through phospholipid vesicle membranes by heptapeptide amphiphiles, Org. Biomol. Chem. 2007;5:2423–2432.
39. Schlesinger PH, Ferdani R, Liu J, Pajewska J, Pajewski R, Saito M, Shabany H, Gokel GW. SCMTR: A chloride-selective, membrane-anchored peptide channel that exhibits voltage gating. J. Am. Chem. Soc. 2002;124(9):1848-9.
40. Djedovic N, Ferdani R, Harder E, Pajewska J, Pajewski R, Schlesinger PH, Gokel GW. The C-terminal ester of membrane anchored peptide ion channels affects anion transport. Chem. Commun. 2003;(23):2862-3.
41. Ferdani R, Pajewski R, Djedovic N, Pajewska J, Schlesinger PH, Gokel GW. Anion Transport in Liposomes is Altered by

Changes in the Anchor Chains and the Fourth Amino Acid of Heptapeptide Ion Channels. New J. Chem. 2005;29:673-680.
42. Schlesinger PH, Djedovic NK, Ferdani R, Pajewska J, Pajewski R, Gokel GW. Anchor chain length alters the apparent mechanism of chloride channel function in SCMTR derivatives. Chem. Commun. 2003;(3):308-309.
43. Pajewski R, Pajewska J, Li R, Daschbach MM, Fowler EA, Gokel GW. The Effect of Midpolar Regime Mimics on Anion Transport Mediated by Amphiphilic Heptapeptides. New J. Chem. 2007;31: 1960-1972.
44. Pajewski R, Ferdani R, Pajewska J, Djedovic N, Schlesinger PH, Gokel GW. Evidence for dimer formation by an amphiphilic heptapeptide that mediates chloride and carboxyfluorescein release from liposomes. Org. Biomol. Chem. 2005;3:619-625.
45. Elliott EK, Daschbach MM, Gokel GW. Aggregation behavior and dynamics of synthetic amphiphiles that self-assemble to anion transporters, Chem. Eur. J. 2008;14: 5871-5879.
46. You L, Ferdani R, Li R, Kramer JP, Winter REK, Gokel GW, Carboxylate anion diminishes chloride transport through a synthetic, self-assembled transmembrane pore, Chemistry – A European Journal, 2008; 14(1):382-396.
47. Schlesinger PH, Ferdani R, Pajewska J, Pajewski R, Gokel GW. Replacing proline at the apex of heptapeptide-based chloride ion transporters alters their properties and their ionophoretic efficacy, New Journal of Chemistry. 2003;26:60-67.
48. Pajewski R, Pajewska J, Li R, Fowler EA, Gokel GW. The Effect of Midpolar Regime Mimics on Anion Transport Mediated by Amphiphilic Heptapeptides New J. Chem. 2007;31:1960–1972.
49. Pajewski R, Ferdani R, Schlesinger PH, Gokel GW. Chloride complexation by heptapeptides: influence of C- and N-terminal sidechains and counterion Chem. Commun. 2004;160-161.
50. Grant GA. Synthetic Peptides: A User's Guide; Second edn; Oxford University Press: Oxford. 2002;390.
51. Ferdani R, Pajewski R, Djedovic N, Pajewska J, Schlesinger PH, Gokel GW. Anion Transport in Liposomes Responds to Variations in the Anchor Chains and the Fourth Amino Acid of Heptapeptide Ion Channels, New J. Chem. 2005;29:673–680.
52. McNally BA, Koulov AV, Smith BD, Joos J-B, Davis AP. A fluorescent assay for chloride transport; identification of a synthetic anionophore with improved activity. Chem. Commun. 2005;1087-1089.
53. Negin S, Gokel MR, Patel MB, Sedinkin SL, Osborn DC, Gokel GW. The Aqueous Medium-Dimethylsulfoxide Conundrum in Biological Studies, RSC-Advances. 2015;5: 8088–8093.
54. Notman MR, Noro B, O'Malley JA. Molecular basis for dimethylsulfoxide (DMSO) action on lipid membranes, J. Am. Chem. Soc. 2006; 128:13982–13983.
55. Notman RWK, den Otter MG, Noro WJ, Briels JA. Thepermeability enhancing mechanism of DMSO in ceramide bilayers simulated by molecular dynamics, Biophys. J. 2007;93:2056–2068.
56. Minooie F, Martin MD, Fried JR. Electro-physiological measurements reveal that a succinyl linker enhances perform-ance of the synthetic chloride channel SCMTR, Chem. Commun. 2018;54:4689 4691.
57. Cook GA, Pajewski R, Aburi M, Smith PE, Prakash O, Tomich JM, Gokel GW. NMR structure and dynamic studies of an anion-binding, channel-forming heptapeptide, J. Am. Chem. Soc. 2006;128:1633-1638.
58. Schlesinger PH, Ferdani R, Pajewski R, Pajewska J, Gokel GW. A hydrocarbon anchored peptide that forms a chloride-selective channel in liposomes, Chem. Commun. 2002;840-1.
59. Clinical and Laboratory Standards Institute: M07-A9, "Methods for dilution antimicrobial susceptibility tests for bacteria that grow aerobically;" Approved standard; 2012. [ISBN 1-56238-784-7]
Available:www.clsi.org, Ninth Edition

Peer-review history:
The peer review history for this paper can be accessed here:
http://www.sdiarticle3.com/review-history/50645